Astron. Astrophys. 320, 237–248 (1997)

ASTRONOMY
AND
ASTROPHYSICS

Implication of light metals (Li-Ca) on NLTE model atmospheres of compact hot stars

T. Rauch

Institut für Astronomie und Astrophysik der Universität, D-24098 Kiel, Germany (rauch@astrophysik.uni-kiel.de)
Lehrstuhl Astrophysik der Universität, Am Neuen Palais 10, D-14469 Potsdam, Germany

Received 7 August 1996 / Accepted 10 September 1996

Abstract. We present an investigation about the influence of "light metals", i.e. lithium through calcium (elements 3 – 20), on structure and emergent fluxes of NLTE model atmospheres for hot compact stars (spectral type O with $T_{\rm eff} \gtrsim$40kK).

In contrast to models which are composed only of H, He, C, N, and O, the models which include light metals have a strongly reduced EUV and X-ray flux. Thus, for the calculation of realistic fluxes in these wavelength bands, the inclusion of light metal opacities is indispensable.

The H I and He II line profiles in the optical wavelength range, which are commonly used for the determination of photospheric parameters like effective temperature, surface gravity, and He/H abundance ratio, are affected only marginally and only within their line cores. However, in the case of high resolution, high S/N spectra, these effects are detectable and thus, the light metals can not be neglected.

Key words: stars: atmospheres – stars: early-type – stars: general stars: fundamental parameters

1. Introduction

In the last quarter of this century enormous progress has been made in both observational technique for stellar spectroscopy and spectral analysis by means of model atmospheres.

New telescopes and instruments supply observers with high resolution and high signal-to-noise optical spectra. After the launch of the IUE[1] satellite in early 1978 a huge number of UV spectra became available and many important metal lines could be analyzed. Satellites like ROSAT[2], HST[3], and EUVE[4] provide additional spectra of the high energy region. Projects like the ESO VLT[5] and the ISO[6] (launched 1995) will improve observations issuing a challenge to spectral analysis which has to be able to interpret the complete spectral range from the far infrared to the X-ray region.

For stars with spectral type B or later LTE model atmospheres are an adequate spectroscopic tool to determine photospheric parameters like effective temperature $T_{\rm eff}$, surface gravity g, and element composition. Fully line blanketed model atmospheres have been presented by Kurucz (1979, 1991, 1992). They include the blanketing effect of hundreds of millions of metal lines. However, there are always NLTE effects in any star which are easily detectable if high-resolution high-S/N spectra, especially of the high energy wavelength range (UV, EUV, X-ray), are evaluated: in the case of the sun these effects were studied e.g. by Sedlmayr (1973, NLTE calculations of the radiative transfer: deviation from LTE of 30-40% for O I λ7773Å, $\approx$20% for O I λ8446Å), Gehren (1975, a few percent larger equivalent widths of Na I lines compared to LTE calculations), Steenbock & Holweger (1984, almost negligible changes of Li I lines, same result for halo dwarfs but larger differences of a factor $\approx$ 2 in the case of supergiants). Recently, NLTE calculations for the sun were presented by Takeda (1995, O I and Na I) and Holweger (1996, Fe I). Rentzsch-Holm (1996) calculated NLTE abundance correction factors for C and Fe in A-type stars and concluded that for a reliable analysis of specific parameters like $T_{\rm eff}$, log g, and metallicity detailed NLTE calculations are necessary.

In case of hot stars ($T_{\rm eff} \gtrsim$30kK) the interpretation of spectra with model atmosphere techniques was hampered by an inadequacy of then existing numerical methods and computational capacity available at that time because NLTE effects have to be considered.

In the "classical" complete linearization (CL) approach (Auer & Mihalas 1969) only rudimentary model atoms and very coarse frequency grids could be used to compute an atmosphere: Auer & Mihalas (1969) calculated pure hydrogen models with a 16-level H I model ion, allowing the lowest five levels to depart from LTE. Six line transitions between the lowest four levels were considered. Models with helium in addition were presented by Auer & Mihalas (1972; He I and He II ground-

[1] International Ultraviolet Explorer
[2] Röntgensatellit
[3] Hubble Space Telescope
[4] Extreme Ultraviolet Explorer
[5] Very Large Telescope
[6] Infrared Space Observatory

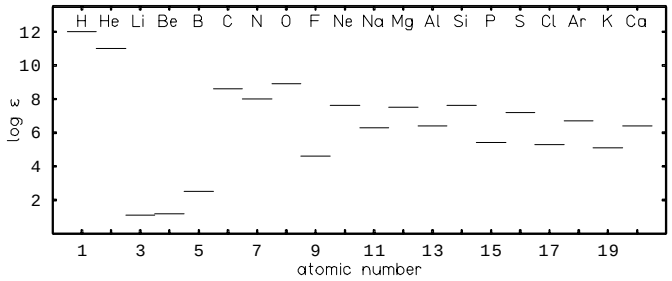

Fig. 1. Solar abundances of the elements 1 – 20, normalized to $\log \sum_i \mu_i \epsilon_i = 12.15$ (Holweger 1979, Stürenburg & Holweger 1990)

states in NLTE) and Kudritzki (1976; lowest six levels of He I and He II in NLTE).

A first attempt to consider carbon, nitrogen, and oxygen approximately in NLTE model atmosphere calculations was made by Mihalas (1972) who included an "average light element": A model atom (five ionization stages with one level each) had been constructed by using average atomic properties of C, N, and O (the most abundant elements besides H and He, Fig. 1).

Husfeld et al.(1984) improved this approach with more detailed calculations of C, N, and O opacities. He constructed simple model atoms (without line transitions) and allowed the ground-states of each ionization stage to depart from LTE.

A newly developed numerical method based on accelerated lambda iteration (ALI) techniques (Werner & Husfeld 1985, Werner 1986, for a review see Hubeny 1992) allows for the calculation of more realistic model atmospheres including effects of metal line blanketing (Werner 1988). Detailed model atoms (for H, He, C, N, O) have been developed in order to carry out precise analyses of optical and UV spectra of hot subdwarfs (e.g. Rauch et al.1991, Rauch & Werner 1991, Rauch 1993). In these "state-of-the-art" model atmospheres more than 200 atomic levels can simultaneously be treated in NLTE and more than 1000 line transitions are considered in detail.

Recently, a hybrid complete linearization / accelerated lambda iteration method (CL/ALI) which combines the merits of both, was presented by Hubeny & Lanz (1993, 1995).

For a long time the spectral analysis was hampered by the lack of atomic data (collisional and photoionization cross-sections, oscillator strengths, line broadening, etc.). The "Opacity Project" (henceforth OP, Seaton 1987, Seaton et al.1992, Seaton et al.1994) as well as the work of Kurucz (1991, 1992) constitute an essential data source. Such data were e.g. used by Dreizler & Werner (1993) in order to interpret EUV spectra. They developed a method to calculate metal line blanketed NLTE model atmospheres which include iron group elements (scandium through nickel) self-consistently.

While the implication of H, He, C, N, and O (Werner 1988, Rauch & Werner 1988, Werner et al.1991, Lanz & Hubeny 1995) and of the iron group elements (Dreizler & Werner 1993, Lanz & Hubeny 1995, Haas et al.1996) on NLTE model atmospheres have been studied in detail, the "light metals" lithium, beryllium, borium, and fluor through calcium have been regarded as trace elements and were neglected in our NLTE model atmosphere calculations so far.

For some of the light metals, line formation calculations (i.e. disregarding atmospheric structure) had been performed: Kamp (1973) carried out Si line formation based on H+He NLTE models ($T_{\rm eff} = 25 - 40$kK, $\log g = 4$) for early-type main-sequence atmospheres. He included continuous opacities of C, N, O, and Ne. For the temperature determination of B stars, NLTE line formation calculations for Si II, Si III, and Si IV have been presented by Becker & Butler (1990a, 1990b). In order to determine their photospheric abundances, Dreizler (1993) carried out line formation calculation for neon, magnesium, and silicon in extremely helium-rich sdO stars (based on H+He+C+N models, $T_{\rm eff} = 43 - 47$kK, $\log g = 5.0 - 6.2$).

However, the "total abundance" of the "light metals" is comparable to that of the CNO elements (Fig. 1) and thus, not negligible in NLTE model atmosphere calculations.

For "cool" stars (type B and later) Anderson (1990) and Grigsby et al.(1992) carried out NLTE model calculations including several millions of atomic transitions of elements with atomic numbers 1 - 28 using the multi-frequency/multi-gray (MF/MG) algorithm.

For "hot" stars, an examination of implication of metals from lithium, beryllium, borium, and fluor through calcium on NLTE model atmospheres was still outstanding. Such a study is presented in this paper.

2. NLTE model atmospheres

The model atmospheres were calculated with the Kiel NLTE model atmosphere code (Werner 1986, 1989). They are plane-parallel, chemically homogeneous, and in hydrostatic and radiative equilibrium. Some details about the construction of the model atoms which were used in the calculations, atomic data, etc. are described in this section.

A set of model parameters $T_{\rm eff}$ and g was selected representing an evolutionary track for a hydrogen-burning post-AGB star (Fig. 2). In the following the model parameters are coded, e.g. M 15565 stands for $T_{\rm eff} = 155$kK and $\log g = 6.5$ (cgs). The abundances of all elements are assumed to be solar. The term Li – Ca denotes in the following the light metals without C, N, and O.

In order to compare their temperature structure, emergent fluxes, and theoretical line profiles of H I and He II, we calculated four model series with different element composition (H, H+He, H+He+C+N+O, H-Ca). The H-Ca models were calculated with three different types of photoionization cross-sections for Li – Ca (Sect. 2.2).

Our hottest model (M 15565) was used to investigate the influence of metal resonance lines on the atmosphere. All other models do not include line opacities of the elements Li – Ca.

2.1. Model atoms and atomic data

In the construction of our model atoms we have to consider that the total number of NLTE levels is restricted to $\approx$ 200 due to numerical accuracy.

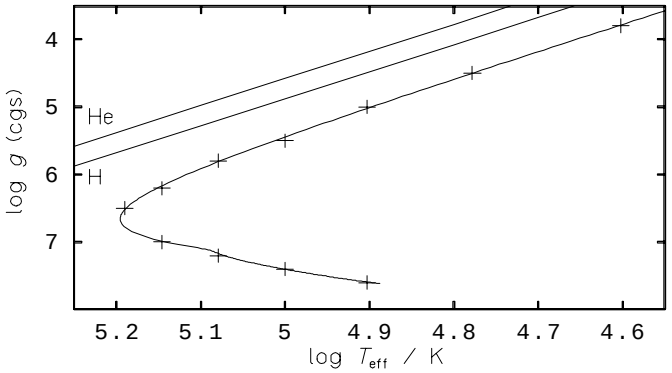

Fig. 2. Position of our models in the log $T_{\rm eff}$ - log g diagram compared to a post-AGB evolutionary track (M = 0.605M$_\odot$) of Schönberner (1983). Additionally shown are the Eddington limits for pure hydrogen (H) and pure helium (He) atmospheres

One of the aims of this work is to check changes of theoretical line profiles of H I and He II which are used in spectral analysis due to the inclusion of light metals in model atmospheres. Thus, we use standard model ions (Rauch & Werner 1988) for H I (10 NLTE levels + 6 LTE levels, 45 line transitions between the NLTE levels) and He II (10 NLTE levels + 22 LTE levels, 45 line transitions). For He I we used two different model ions for $T_{\rm eff}$ < 100kK and $T_{\rm eff}$ ≥ 100kK (19/5 NLTE levels + 17/21 LTE levels with 34/8 line transitions, respectively).

The selection of some (lower) NLTE and some (higher) LTE levels as well as the cutoff at a certain total number of levels appears to be somewhat arbitrary. In the case of H I, it is the result of the "classical" number of 16 levels used by Auer & Mihalas (1969) and an investigation by Rauch & Werner (1988) about the influence of the number of levels treated in NLTE on the model atmosphere: They found that at least eight NLTE levels are necessary in order to achieve an accuracy better than 1% in the emergent line fluxes.

A more accurate approach which eliminates the necessity of this cutoff has been presented by Hubeny et al.(1994). They generalized the occupation probability formalism of Hummer & Mihalas (1988, HMF) to NLTE conditions. Using exact partition functions, they have shown that the number of levels is no more an indicator for the accuracy of a model.

Differences were found by Hubeny et al.(1994) in the case of $T_{\rm eff}$ = 20, 35kK, log g = 4 models and by Werner (1996) in the case of a $T_{\rm eff}$ = 82kK, log g = 6.2 model (at solar abundances) if the HMF is employed. Thus, for the calculation of realistic models used for spectral analyses, the use of the HMF is highly recommended. However, this work started before our NLTE code has been updated on the HMF and thus, we calculated all models without the HMF.

C, N, and O are represented by small model atoms (Table 1). Bues & Aslan (1995) have shown that in the case of a LTE model atmosphere ($T_{\rm eff}$ = 60kK, log g = 7.5) which is composed of H, He, and C with solar abundance ratios, the emergent flux shortward the C V ground-state edge (31.6Å) is reduced by at least eight orders of magnitude. In the case of hotter LTE model

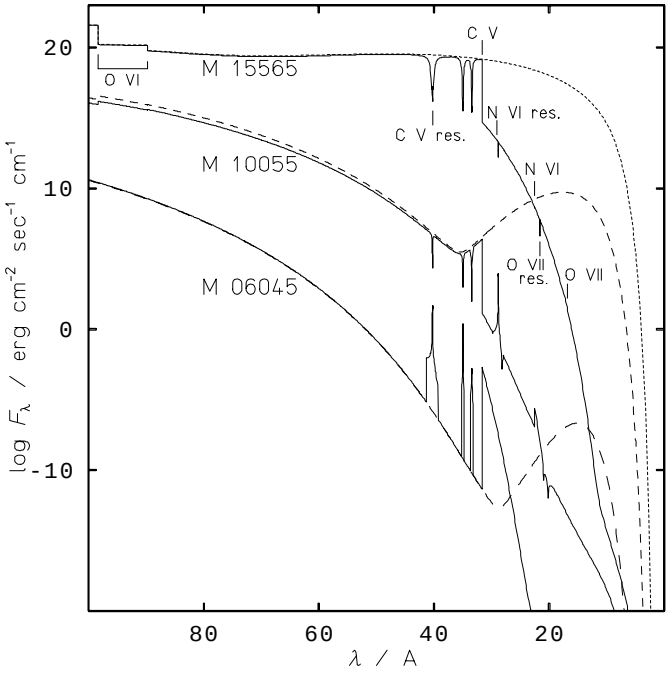

Fig. 3. Emergent fluxes of models M 06045, M 10065, and M 15565 (H+He+C+N+O). For the calculation we used our standard model atoms (Table 1, - - -) and model atoms which are extended to higher ionization stages: C VI, N VII, and O VIII (——). Note that the C V ground-state threshold and the C V resonance lines appear in emission in M 06045. The same is found for N VI in M 10055. N VI is not considered in detail in M 06045, O VII is only considered (in detail) in M 15565

atmospheres ($T_{\rm eff}$ < 600 kK, log g = 8), Heise et al.(1994) found that the dominant absorption edges are due to C V and C VI. In order to investigate the necessity to consider C VI, N VII, or O VIII, we calculated exploratory models (H+He+C+N+O) with extended model atoms. In Fig. 3 we compare the emergent fluxes of these models with that of our "standard" models.

In our "extended" model (M 15565), the flux shortward the C V ground-state absorption edge is reduced by about five orders of magnitude and the C V resonance series is clearly detectable. The N VI and O VII absorption edges as well as the respective resonance lines are weak. In M 10055, the N VI ground-state threshold appears in emission while the C V ground-state threshold is still in absorption. In M 06045 this turns into emission, too. Note, that the strong C V ground-state absorption occurs at a flux level which is about 2, 14, and 20 magnitudes below the maximum flux level in the models M 15565, M 10055, and M 06045, respectively. As a consequence, the temperature structures of these models differ only marginally.

The ionization fractions of C, N, and O (M 15565) are shown in Fig. 4. While C VI dominates the innermost and outermost atmosphere layers, the isoelectronic N VII and O VIII are unimportant.

We conclude that C V must be included in model atmosphere calculations in order to analyze X-ray data (Rauch 1996), but

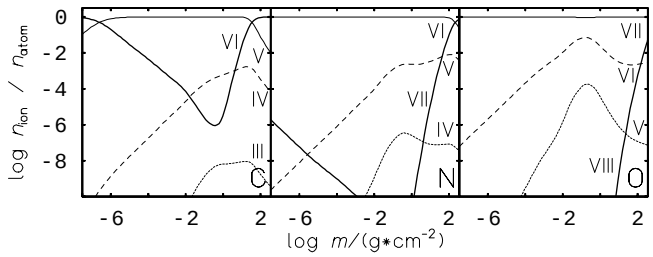

Fig. 4. Ionization fractions of C, N, and O in M 15565 (H+He+C+N+O), calculated with extended model atoms

restrict in the following to the small model atoms and disregard the high CNO ionization stages.

The model atoms for Li – Ca are build as large as possible. It is clear that we can not include detailed model atoms with many line transitions but we want to consider at least the resonance lines because they will probably have an influence on the temperature stratification (Rauch & Werner 1991, Rauch 1993, Werner 1996). Following Rauch (1993), we used an approximate formula for the calculation of the absorption coefficients of these lines in order to account for the Stark effect. These lines are represented in the frequency grids for a minimum of 1 000 thermal Doppler widths. For the complete Lyman and Balmer series of H I and He II, the Stark effect is considered, too.

For proper model atoms, the dominant ionization stages of all elements in the line forming region were determined in test calculations before. For our hottest model (M 15565) the ionic fractions are shown in Fig. 5.

In the model atmosphere calculations the dominant ionization stages are represented by a few NLTE levels whereas for other ionization stages only one NLTE level is included.

In test calculations we did not find any implication of Li, Be, and B on the atmospheres — not even absorption edges in the emergent flux. These elements are more than 100 times less abundant (Fig. 1) than the other light metals. Thus, we neglected these elements in our further calculations.

The statistics of the model atoms of all elements included in our model atmosphere calculations are summarized for two selected model atmospheres in Table 1.

The Opacity Project atomic database "TOPbase" (Cunto & Mendoza 1992) at the CDS (Strasbourg, France) gives access to an extensive dataset of energies, photoionization cross-sections ($\sigma_{\rm bf}$), and oscillator strengths of elements with atomic numbers 1 - 14, 16, 20, and 26. Hence, model atoms for these elements can easily be constructed.

Since there are discrepancies in observed and OP (calculated) level energies, energies are partly substituted by values given in Bashkin & Stoner (1975) in order to yield more exact threshold and line positions.

For elements which are not considered in the OP, we used data from standard sources (e.g. Bashkin & Stoner 1975, Moore 1971, Wiese et al.1966, Wiese et al.1969). The $\sigma_{\rm bf}$ are calculated hydrogen-like ($\sigma_{\rm bf}^{\rm H}$, Sect. 2.2), in this case.

Table 1. Statistics of the models atoms used in our calculations for two selected models. The notation is: NLTE = levels treated in NLTE, LTE = LTE levels, RBB = radiative bound-bound transitions

		M 04038			M 15565		
atom	ion	NLTE	LTE	RBB	NLTE	LTE	RBB
H	I	10	6	45	10	6	45
	II	1	-	-	1	-	-
He	I	19	17	34	5	21	8
	II	10	22	45	10	22	45
	III	1	-	-	1	-	-
C	III	3	64	1	3	64	1
	IV	5	11	6	5	11	6
	V	1	0	0	5	28	3
	VI	-	-	-	1	0	0
N	II	2	20	0	-	-	-
	III	5	40	3	1	44	1
	IV	3	91	1	3	91	1
	V	1	0	0	5	15	6
	VI	-	-	-	1	0	0
O	II	2	3	0	-	-	-
	III	5	49	1	-	-	-
	IV	1	0	0	4	7	3
	V	-	-	-	5	7	6
	VI	-	-	-	5	6	1
	VII	-	-	-	1	0	0
F	II	1	19	0	-	-	-
	III	4	19	0	-	-	-
	IV	2	10	0	-	-	-
	V	1	0	0	3	6	1
	VI	-	-	-	3	4	1
	VII	-	-	-	2	4	1
	VIII	-	-	-	1	0	0
Ne	II	2	27	0	-	-	-
	III	3	34	0	-	-	-
	IV	4	42	0	4	6	1
	V	1	0	0	9	4	4
	VI	-	-	-	8	15	9
	VII	-	-	-	10	35	12
	VIII	-	-	-	1	0	0
Na	II	1	21	0	-	-	-
	III	2	37	0	-	-	-
	IV	5	5	0	1	4	0
	V	1	0	0	4	4	1
	VI	-	-	-	5	7	1
	VII	-	-	-	4	7	2
	VIII	-	-	-	1	0	0
Mg	II	2	6	0	-	-	-
	III	4	15	0	-	-	-
	IV	5	9	0	1	13	0
	V	1	0	0	5	16	2
	VI	-	-	-	4	4	1
	VII	-	-	-	5	7	1
	VIII	-	-	-	1	0	0
Al	III	1	6	0	-	-	-
	IV	4	13	0	1	16	0
	V	1	0	0	5	12	3
	VI	-	-	-	5	15	3
	VII	-	-	-	4	3	1
	VIII	-	-	-	1	0	0
Si	III	2	11	0	-	-	-
	IV	3	4	0	1	6	0
	V	4	12	0	4	12	2
	VI	1	0	0	2	1	1
	VII	-	-	-	4	3	1
	VIII	-	-	-	1	0	0
P	III	2	8	0	-	-	-
	IV	3	3	0	-	-	-
	V	3	1	0	3	9	2
	VI	1	0	0	3	2	2
	VII	-	-	-	2	2	1
	VIII	-	-	-	1	0	0

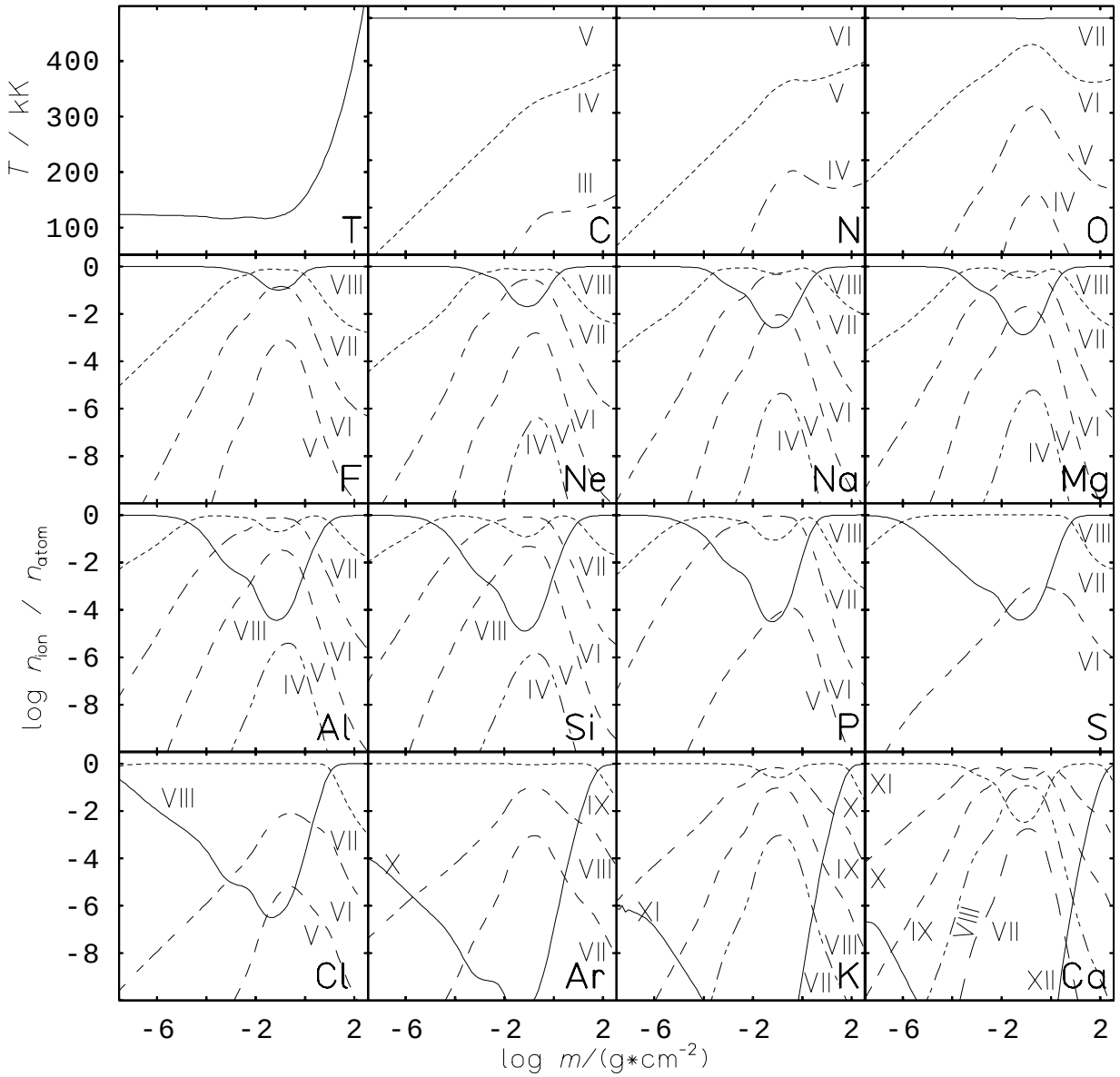

Fig. 5. Temperature structure (T) and ionization fractions of the elements C – Ca in model M 15565

2.2. Photoionization cross-sections

For the $\sigma_{\rm bf}$ of H, He, C, N, and O we used the same values like Rauch (1993). Cross-sections for the other metals are calculated in three different ways:

- $\sigma_{\rm bf}^{\rm H}$ The $\sigma_{\rm bf}$ are calculated hydrogen-like, i.e. we used the Seaton formula (Seaton 1958) with $s = 3$ and $\alpha = 1$: $\sigma_\nu = \sigma_\circ \left(\nu_{\rm th}/\nu\right)^3$. The threshold cross-section $\sigma_\circ$ is also hydrogen-like (e.g. Mihalas 1978).
- $\sigma_{\rm bf}^{\rm th}$ Same as $\sigma_{\rm bf}^{\rm H}$ but the threshold cross-section $\sigma_\circ$ is taken from the OP data.
- $\sigma_{\rm bf}^{\rm OP}$ The OP data set is used.

In Fig. 6 the run of $\sigma_{\rm bf}^{\rm H}$ and $\sigma_{\rm bf}^{\rm OP}$ are compared in case of the Al VI ground-state. In all examined cases for different levels used in our calculations we find the OP data ($\sigma_{\rm bf}^{\rm OP}$) generally to be larger than the hydrogen-like ($\sigma_{\rm bf}^{\rm H}$) values by approximately one order of magnitude. The difference in the emergent fluxes calculated from models which consider either $\sigma_{\rm bf}^{\rm H}$, or $\sigma_{\rm bf}^{\rm th}$, or $\sigma_{\rm bf}^{\rm OP}$ cross-sections is shown in Fig. 10.

2.3. Frequency grids

Our frequency grids cover the interval $\left[1 \cdot 10^{12}, 3 \cdot 10^{18}\right]$ Hz. They include points for thresholds, line transitions, and "continuum" points.

Additional continuum points were added in order to investigate whether an "exact" representation of OP photoionization cross-sections (Sect. 2.2), i.e. resolving narrow resonances, has an influence on the model atmosphere or not. For this purpose

Table 1. (continued)

		M 04038			M 15565		
atom	ion	NLTE	LTE	RBB	NLTE	LTE	RBB
S	III	1	9	0	-	-	-
	IV	3	12	0	-	-	-
	V	3	17	0	-	-	-
	VI	3	9	0	3	9	2
	VII	1	0	0	6	32	4
	VIII	-	-	-	1	0	0
Cl	III	1	9	0	-	-	-
	IV	3	8	0	-	-	-
	V	3	4	0	-	-	-
	VI	3	5	0	3	5	1
	VII	1	0	0	3	5	1
	VIII	-	-	-	3	4	2
	IX	-	-	-	1	0	0
Ar	III	2	15	0	-	-	-
	IV	4	21	0	-	-	-
	V	5	30	0	-	-	-
	VI	4	11	0	-	-	-
	VII	1	0	0	3	17	1
	VIII	-	-	-	3	6	2
	IX	-	-	-	4	2	2
	X	-	-	-	1	0	0
K	III	1	8	0	-	-	-
	IV	3	16	0	-	-	-
	V	3	4	0	-	-	-
	VI	3	3	0	-	-	-
	VII	1	0	0	1	13	0
	VIII	-	-	-	4	10	1
	IX	-	-	-	3	4	2
	X	-	-	-	1	0	0
	XI	-	-	-	1	0	0
Ca	III	1	16	0	-	-	-
	IV	3	6	0	-	-	-
	V	5	18	0	-	-	-
	VI	4	12	0	-	-	-
	VII	1	0	0	5	12	1
	VIII	-	-	-	3	6	1
	IX	-	-	-	3	17	1
	X	-	-	-	3	9	2
	XI	-	-	-	4	28	2
	XII	-	-	-	1	0	0
	total	196	858	136	225	719	197

equidistant ($\Delta\lambda$ = 0.1Å) points within 230Å$\geq\lambda\geq$5Å were set. It is worth to mention here that the energy of a resonance depends on the energies of the levels used for the calculation. Since the level energies are also calculated within the frame of the OP (Sect. 2.1), the resonance's energies can differ from observation as well as the energies do. However, our test calculations have shown that the additional frequency points have only a small influence on the model structure and thus, it is not necessary to include them during the model atmosphere calculation. Moreover, the exact position of the resonances does not matter for the computed atmospheric structure.

For the calculation of the emergent fluxes (Fig. 12) however, we have to include them and hence, we decided to include them in our model atmosphere calculations, too. A typical frequency grid contains about 7 500 frequency points.

3. Atmospheric structure

The temperature structure of a model atmosphere is an indicator for the elements which are considered as well as for the model atoms used in the calculation (e.g. Rauch & Werner 1988, Rauch et al.1991). In the case of the sdO star KS 292 ($T_{\rm eff}$ = 75kK, $\log g$ = 5.0), a drastic temperature drop was found in the outer atmosphere due to desaturating resonance lines of C IV and N V by Rauch et al.(1991).

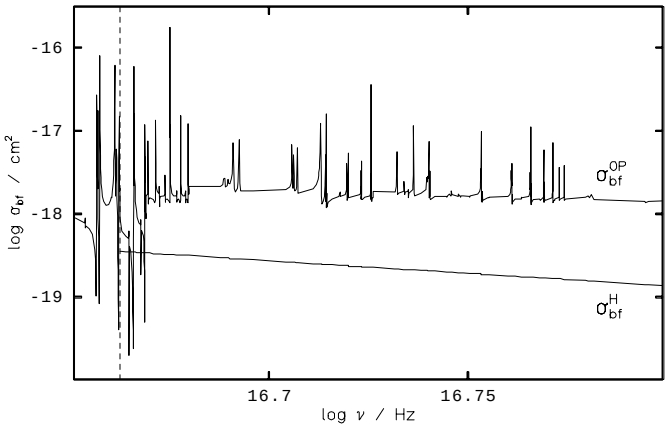

Fig. 6. Comparison of hydrogenic and Opacity Project photoionization cross-sections of the Al VI ground-state. The dashed line indicates the ionization frequency ($\nu_{\rm th}$)

In Fig. 7 we compare the temperature stratification of models with $T_{\rm eff}$ = 40, 80, 120, 155 kK, and increasing number of elements. While the inner atmosphere ($\log m$>0) remains almost unchanged in all models, we find significant changes in the outer atmosphere. The influence of the different photoionization cross-sections (Sect. 2.2) for the light metals on the temperature is small (model M 15565).

An extreme temperature drop of about 40 kK occurs in the outer layer of model M 15565 if we include the resonance lines of F – Ca. A similar effect can be expected in other models but we have not calculated further "line" models because their calculation requires a lot of computational time (Sect. 4) and is out of the scope of this paper. However, in future models which include light metals and are used for spectral analysis this has to be checked in detail.

In Fig. 8 the influence of individual elements is shown: Due to their higher abundances (relative to the other light metals), the largest changes in the temperature stratification are due to Ne, Mg, and Si. The resonance lines of their dominating ionization stages form far out in the atmosphere (Fig. 7) and, while desaturating, strongly cool it. F is totally negligible and the other light metals have only a marginal influence (in Fig. 7 the temperature structure which is calculated with all elements F – Ca is shown).

The drastic temperature drop affects the ionization equilibria of all elements (Fig. 9). It extends into the atmosphere down to $\log m \approx -1.3$ and thus includes the H/He line forming regions $-2.5 \lesssim \log m \lesssim -1.3$ which are important for spectral analyses (Sect. 5). Werner (1996) has shown that this is one of the reasons for the so-called Balmer line problem found in H-He model atmospheres (e.g. Napiwotzki & Rauch 1994): in our H-He models, we find an increasing temperature at the formation depths of the Balmer series towards H α, whereas in our H-Ca models

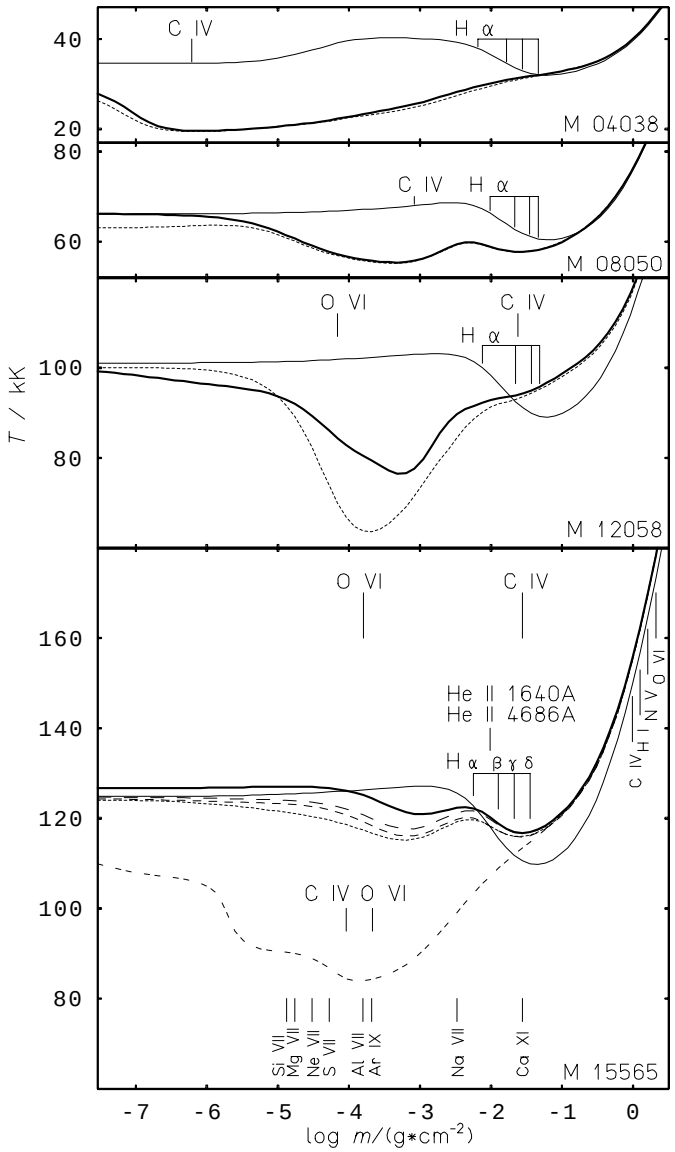

Fig. 7. Temperature structures of M 04038, M 08050, M 12058, and M 15565 (—: H+He, **—**: H+He+C+N+O, — — —: H-Ca + $\sigma_{\rm bf}^{\rm H}$, – – –: H-Ca + $\sigma_{\rm bf}^{\rm th}$, - - -: H-Ca + $\sigma_{\rm bf}^{\rm OP}$, -- --: H-Ca with $\sigma_{\rm bf}^{\rm OP}$ + F-Ca resonance lines. The formation depths of the line cores of H α – H δ, He II $\lambda\lambda$ 1640, 4686Å, the C IV and O VI resonance lines, and of the ground-state thresholds of H I, C IV, N V, and O VI (H-Ca with $\sigma_{\rm bf}^{\rm OP}$) are marked. The formation depths of some resonance lines of F-Ca are marked for the H-Ca ($\sigma_{\rm bf}^{\rm OP}$) model which was calculated with all resonance lines. Note that the C IV resonance line forms much further outside in this model (lower labels) compared to the model calculated without the F-Ca resonance lines

we find that this temperature is decreasing. In Sect. 5 we show the resulting theoretical line profiles.

4. Emergent fluxes

The emergent flux is a sensitive indicator for the presence of metals in the photosphere. In Fig. 10 we compare fluxes calculated from models (M 15565) with different element composition. The CNO opacities reduce strongly the flux at energies

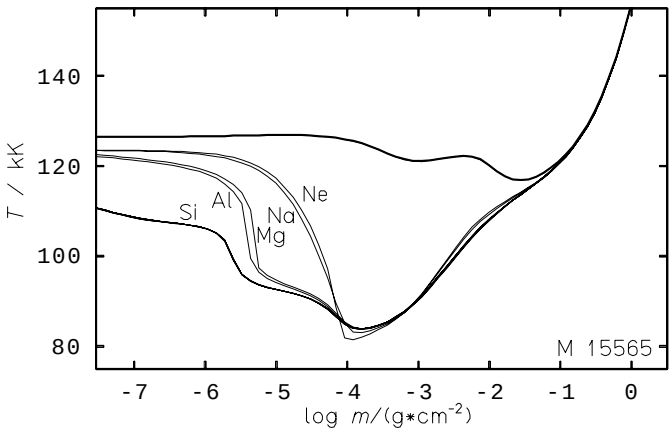

Fig. 8. Influence of individual elements on the temperature structure of the hottest model (M 15565). The thick line represents the stratification of the H+He+C+N+O model, the light metals are added subsequently (in order of their atomic number). The labels indicate the last element which is considered

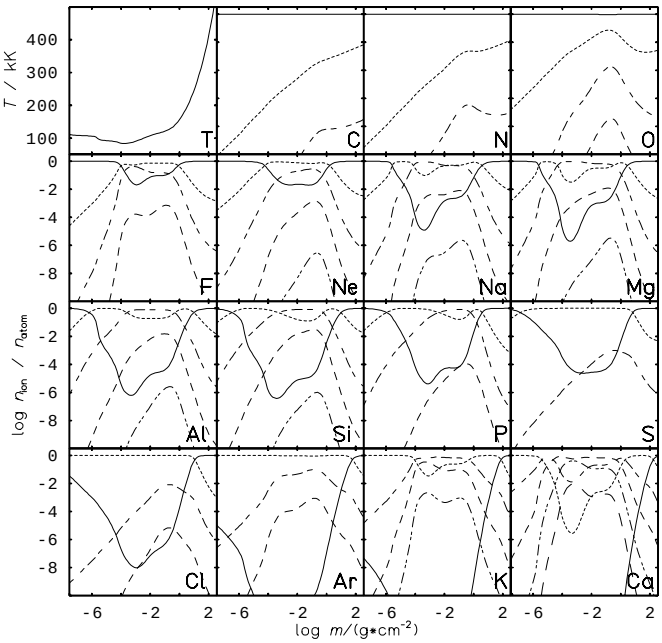

Fig. 9. Same as Fig. 5. In the model calculation we considered the resonance lines of F – Ca. Note that changes in the ionization equilibria are found in the outer atmosphere at $\log m \lesssim -1.3$ which includes the line-forming regions (Fig. 7)

higher than the O VI 2p edge (λ <98 Å). The opacities of F-Ca reduce the flux even more but at higher energies. The comparison of the fluxes calculated with $\sigma_{\rm bf}^{\rm H}$, $\sigma_{\rm bf}^{\rm th}$, and $\sigma_{\rm bf}^{\rm OP}$ shows a huge difference: at $\lambda \approx$20 Å, $\sigma_{\rm bf}^{\rm OP}$reduces the flux by about ten orders of magnitude stronger than $\sigma_{\rm bf}^{\rm H}$.

The influence of the light metals on the emergent fluxes of models with different $T_{\rm eff}$ is shown in Fig. 11.

No prominent absorption egde of the light metals can be detected in the fluxes calculated from the H-Ca models at so-

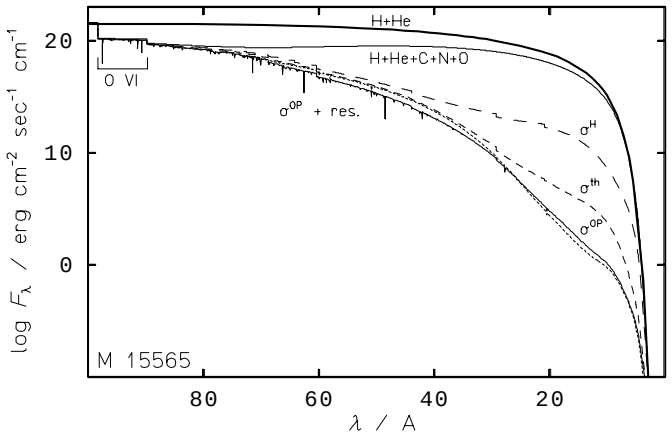

Fig. 10. Emergent fluxes of M 15565 models with different element composition (solar abundances). ▬: H+He, ——: H+He+C+N+O, — — —: H-Ca with $\sigma_{\rm bf}^{\rm H}$, – – –: H-Ca with $\sigma_{\rm bf}^{\rm th}$, - - -: H-Ca with $\sigma_{\rm bf}^{\rm OP}$, ——: H-Ca with $\sigma_{\rm bf}^{\rm OP}$ and additionally all resonance lines of F-Ca. Note the logarithmic flux scale: in the case of H-Ca with $\sigma_{\rm bf}^{\rm OP}$, at 50 Å the model flux with resonance lines is reduced by a factor of 8

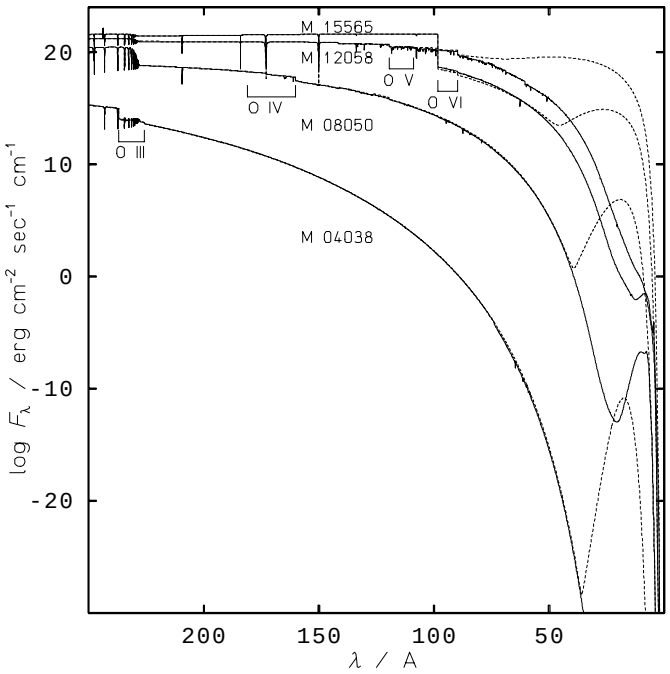

Fig. 11. Comparison of emergent fluxes of H+He+C+N+O (- - -) models with fluxes of H-Ca models (——, calculated with $\sigma_{\rm bf}^{\rm OP}$, no lines for F-Ca), shown for M 04038, M 08050, M 12058, and M 15565. The most prominent absorption edges are due to oxygen. Significant differences appear only at wavelengths $\lambda < 98$ Å (O VI 2p threshold); at lower $T_{\rm eff}$, they are found far below the maximum flux level

lar abundances — if only one additional species is considered besides H+He+C+N+O, strong absorption edges of it can be identified (Fig. 12).

A similar effect is found if we increase the abundance ratios of all light metals: In Fig. 13 we compare the fluxes of H-Ca models with different abundances. At lower abundances than solar, absorption edges of the highest ionization stages which are dominant in the continuum forming region can be detected. At higher abundances, the flux is already absorbed by the lower ionization stages and thus, these absorption edges are no longer prominent. It is worthwhile to note that in sufficiently hot white dwarfs radiative levitation counteracts gravitational settling and an overabundance (compared to the solar abundances) of the light metals ($\approx$ one order of magnitude) is possible (Chayer et al.1995).

The calculation of NLTE models presented here (with ≈ 200 levels treated simultaneously in NLTE, Table 1) requires quite a lot of computational time which increases tremendously if line transitions of the light metals are included. Due to the extreme non-linearity of the radiation field and the drastic changes in the temperature structure due to the desaturating resonance lines (Fig. 8), the process of convergence has to be damped in order to avoid numerical instabilities. Although we tried hard, we could only calculate one convergent model which considers the metal line blanketing of F – Ca is M 15565. Our models with lower g lie closer to the Eddington limit (Fig. 2) and the resonance lines (e.g. that of C IV) form more outside in the atmosphere (Fig. 7) which results in further instability. The models with higher g require to consider more ionization stages of the heavier elements which has the same effect because small changes in the temperature structure shift the complete ionization equilibrium.

Consequently, we investigate whether classical line formation calculation, i.e. calculation of NLTE occupation numbers at fixed temperature structure may be sufficient. As could be expected from the comparison of the M 15565 models calculated with/without resonance lines of the light metals (Fig. 10), the flux of the line-formation model is on the average much higher than the flux of the "consistent" model (Fig. 14). We conclude that line formation calculations are not sufficient to predict emergent fluxes.

5. Line profiles

The atmospheric structure depends strongly on the element composition and on the model atoms which are used for its calculation. Thus one can expect changes in the theoretical line profiles calculated from the atmosphere. The H I and He II lines are often used to determine photospheric parameters like $T_{\rm eff}$, $\log g$, and the He/H abundance ratio. In Table 2 we summarize the changes in the equivalent widths of some H and He lines calculated from different models.

Regarding the equivalent widths given in Table 2, the additional effect of light metal opacities is, as long as only continua are considered (H-Ca), small compared to the changes between values which are calculated from H+He and H+He+C+N+O models. The same result was found for other H I and He II lines.

The consideration of light-metal line blanketing has a slightly stronger influence on the equivalent widths but the changes in the line profiles are marginal and are found only in the line cores (Fig. 15): The emission reversals of H α and He II λ 4686Å increase. Regarding the strongly reduced tem-

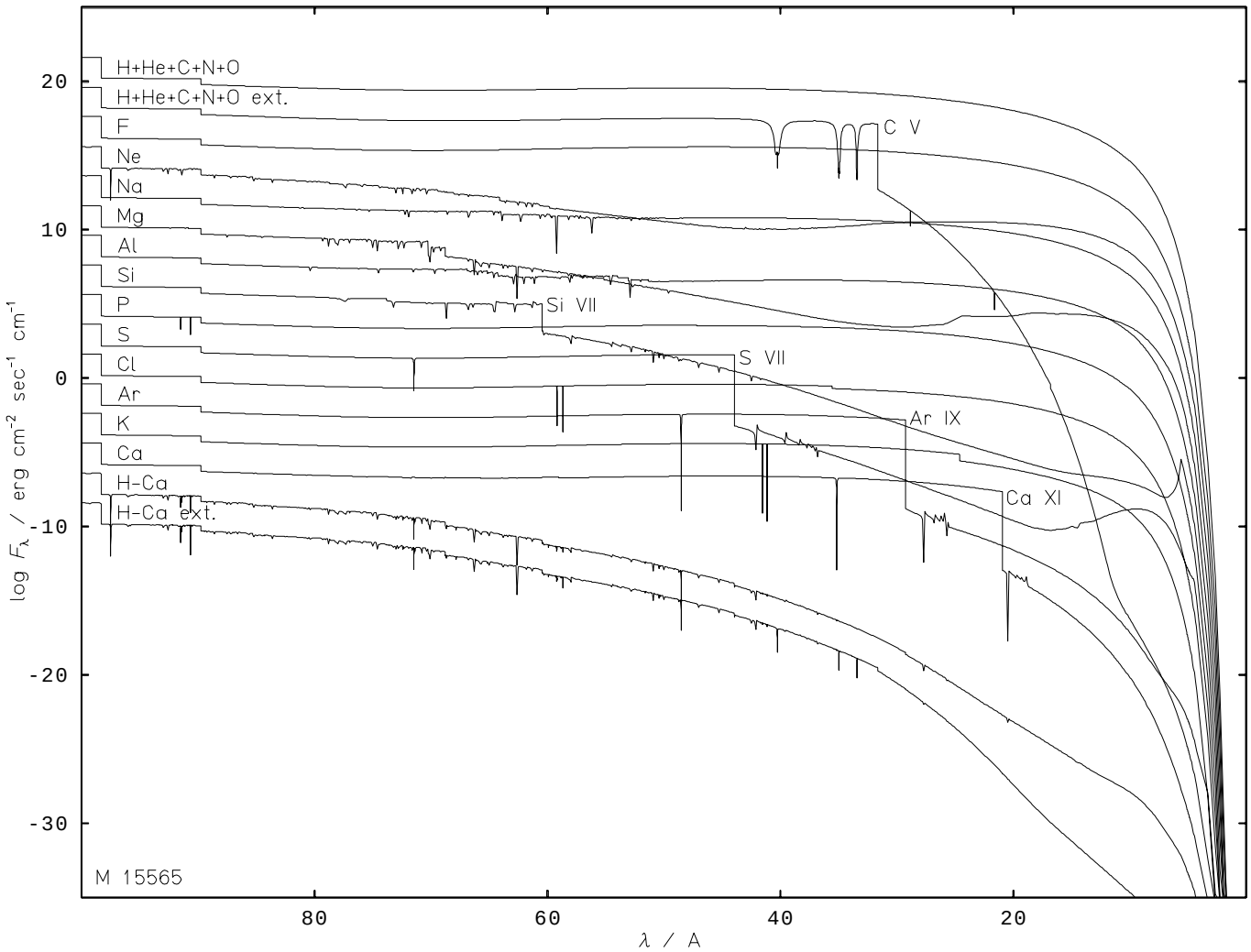

Fig. 12. Comparison of emergent fluxes of our H+He+C+N+O models (M 15565) with fluxes of models with only one additional element (F, Ne, . . ., Ca) considered and with the flux of models in which all elements are considered. "ext." denotes models where an extended C model atom is used (Sect. 2.1). Note the strong absorption edges of C V, S VII, Ar IX, and Ca XI which reduce the flux by about five orders of magnitude. These edges disappear almost in the H-Ca models – but note the logarithmic scale: they still reduce the flux strongly. In the H-Ca ext. model, the influence of the C V opacity is obvious. All models but H+He+C+N+O are vertically shifted in 2 dex steps for sake of clarity

peratures at their formation depths (Fig. 7), this appears counterintuitive but is the result of a higher ratio of the upper/lower level departure coefficients which has a stronger influence than the lower temperature. A similar result was found by Lanz & Hubeny (1995).

In order to investigate the influence of the individual elements on the line profiles of H α and He II λ 4686Å, we calculated their equivalent widths from the models of Fig. 8 (Table 3). As expected, the main effect on these lines in this hot model is due to Ne which is responsible for the strong cooling in the line forming regions (Figs. 7, 8).

6. Discussion and conclusions

The metal opacities have a great influence on the structure of model atmospheres. For the calculation of realistic emergent fluxes in the EUV and X-ray range, the consideration of metals is indispensable: In the case of hot stars ($T_{\rm eff} \gtrsim$40kK) a strong absorption (many orders of magnitude !) of the flux at energies higher than the O VI 2p continuum (126 eV) is found due to the light metals F – Ca.

At solar abundances, Li, Be, and B do not have any influence on the model atmospheres and may be neglected. F, P, Cl, and K have only a very small influence compared to the other light metals (Ne, Na, Mg, Al, Si, S, Ar, Ca). Recent calculations by Chayer et al.(1995) have shown that the photospheric abundances of the light metals may be strongly increased by radiative levitation in very hot white dwarfs. This will effect the emergent flux: a stronger absorption in the X-ray range has to be expected (Fig. 4).

The use of photoionization cross-sections from the Opacity Project instead of a hydrogen-like approximation for the ele-

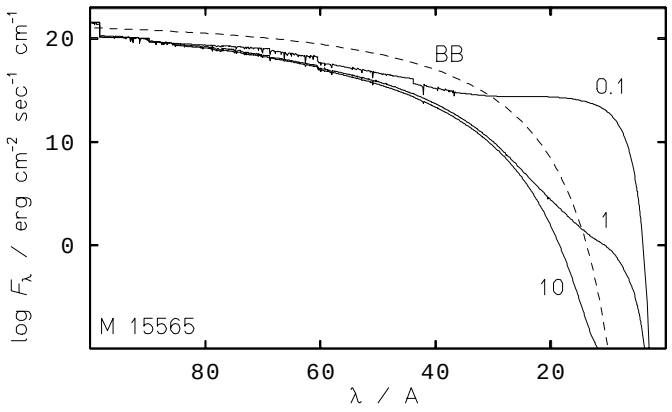

Fig. 13. Comparison of emergent fluxes of H-Ca models (M 15565) calculated with different abundances (0.1, 1, 10×solar) of the light metals. Note that their absorptions edges are clearly detectable only at lower abundances. BB denotes the flux of a black body with T = 155 kK

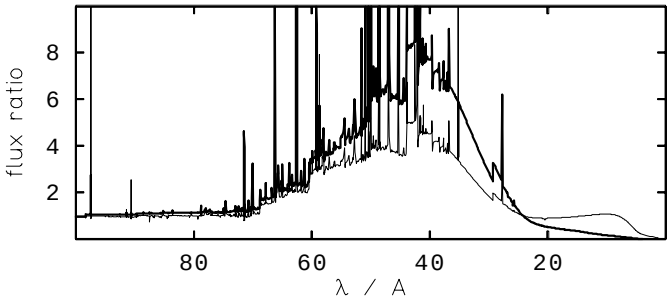

Fig. 14. Flux ratios of M 15565 (H-Ca). Thin line: calculated without / with resonance lines; thick line: line formation calculation / model (both with all resonance lines). The line formation calculation is based on the temperature structure of the H+He+C+N+O model

ments F – Ca results in a much stronger reduction of the EUV and X-ray flux level. These data do not have to be used in great detail, i.e. it is not necessary to consider the resonance structures in the model atmosphere calculation.

The H I and He II lines which are used for the analysis of photospheric parameters like effective temperature, surface gravity, and He/H abundance ratio do not change drastically if light metals are considered, i.e. spectral analyses based on H+He+C+N+O models are sufficient to determine these values reliably. A similar result was found by Haas et al.(1996) in the case of iron group elements. However, the present observational accuracy is of the order of one percent and thus in state-of-the-art NLTE model atmospheres, metals should not be neglected.

The necessity to include metal line blanketing in the atmosphere calculation in order to model the temperature structure is evident in our hottest model ($T_{\rm eff}$ = 155kK) — a classical "line formation" calculation (i.e. calculation of a H-Ca model at a fixed temperature stratification which is taken from a H+He or even H+He+C+N+O model) is not sufficient if high-resolution high-S/N spectra shall be analyzed.

Table 2. Equivalent widths (given in mÅ, the emission parts of the profile contribute with a negative sign) of some theoretical Balmer lines (H α – H δ, with their respective He II blends), and of He II $\lambda\lambda$ 4686, 5411Å calculated from our H+He models, and changes (in %) to these for the same lines calculated from our H+He+C+N+O (H-O), and H-Ca models (in the case of M 15565 also for the model which includes all the resonance lines, L)

model		H α	H β	H γ	H δ	4686	5411
04038	H+He	3442	3261	2846	2599	887	1306
	H-O	-4.0	-3.7	-3.3	-3.1	+7.8	-2.8
	H-Ca	-3.5	-3.5	-3.2	-3.0	+5.0	-3.0
06045	H+He	3658	3413	3018	2801	1344	1545
	H-O	-2.2	-4.4	-4.9	-5.3	+3.8	-3.0
	H-Ca	-1.6	-4.1	-4.7	-5.3	+4.8	-2.7
08050	H+He	3615	3361	2981	2739	1487	1485
	H-O	-2.1	-1.1	-0.7	-0.8	+2.4	+3.7
	H-Ca	-2.2	-1.2	-0.8	-0.9	+2.9	+3.8
10055	H+He	3309	3174	2782	2457	1404	1153
	H-O	-9.3	+0.9	+3.1	+3.3	+1.4	+13.0
	H-Ca	-9.6	+0.3	+2.5	+2.7	+1.1	+12.3
12058	H+He	3215	3063	2607	2189	1244	922
	H-O	+7.7	+5.1	+2.1	-1.8	+18.4	+14.0
	H-Ca	+13.6	+6.5	+2.5	-1.8	+23.4	+12.9
14062	H+He	2947	2825	2347	1862	1018	711
	H-O	+10.3	+8.8	+5.3	+1.1	+14.1	+16.3
	H-Ca	+10.8	+8.0	+4.0	-0.5	+16.6	+13.9
15565	H+He	2721	2618	2139	1621	848	560
	H-O	+11.2	+8.8	+4.3	-0.2	+5.2	+17.3
	H-Ca	+10.6	+9.3	+4.8	+0.1	+10.7	+18.5
	L	+2.1	+14.9	+11.6	+6.6	-17.0	+32.0
14070	H+He	2150	2413	2091	1553	896	674
	H-O	+22.5	+7.5	-3.9	-10.8	+10.9	+4.9
	H-Ca	+24.0	+7.8	-3.8	-10.8	+17.7	+2.2
12072	H+He	2113	2789	2552	1924	1263	983
	H-O	+13.5	+10.4	+6.9	+4.9	+6.8	+15.3
	H-Ca	+10.4	+9.1	+5.8	+3.8	+5.1	+11.9
10074	H+He	2815	4313	4076	3128	2121	1892
	H-O	+12.8	+7.3	+4.8	+3.9	+3.7	+8.2
	H-Ca	+9.5	+7.2	+5.4	+4.5	+5.3	+8.6
08076	H+He	4069	6434	6129	4790	3098	2978
	H-O	-7.4	-10.6	-11.2	-11.7	-9.4	-12.7
	H-Ca	-1.0	-1.7	-2.3	-2.9	-1.0	-1.9

Model atmospheres which consider light metals have successfully been used, e.g. in order to determine the Ne abundance in PG 1159 stars (Werner & Rauch 1994) and to calculate model atmospheres for ultra-hot pre-white dwarfs (Werner et al.1995).

However, for a reliable analysis a precise determination of the photospheric metal abundances is necessary.

Acknowledgements. I would like to thank Klaus Werner for many helpful discussions and careful reading of the manuscript. Computations were carried out on CRAY computers of the Rechenzentrum der Universität Kiel and of the Konrad-Zuse-Zentrum für Information-

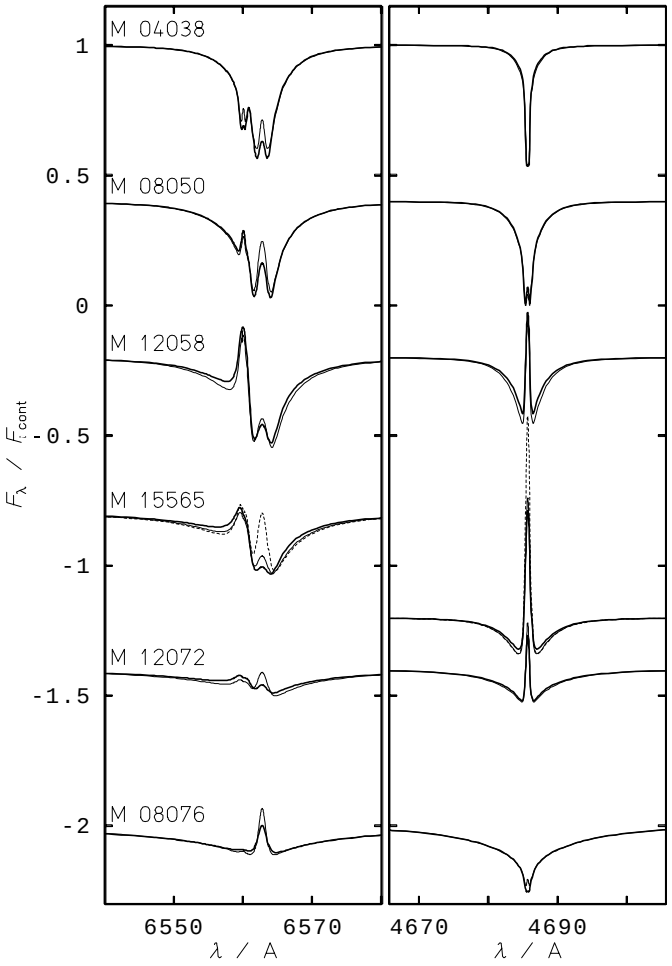

Fig. 15. Theoretical line profiles of the H α - He II blend and of He II λ4686Å calculated from the same models like in Table 2: —: H+He+C+N+O, —: H-Ca, - - - (only in model M 15565): H-Ca with resonance lines of the light metals. Note that the consideration of the resonance lines results in much stronger emission reversals in both, H α and He II λ4686Å

Table 3. Equivalent widths (given in mÅ) of H α (incl. He II blend) and He II λ4686Å calculated from models (M 15565) of Fig. 8

element	H α	4686
H+He+C+N+O	3104	958
F	3105	958
Ne	2766	729
Na	2772	723
Mg	2766	708
Al	2747	706
Si	2783	709
P	2783	709
S	2785	711
Cl	2785	711
Ar	2781	709
K	2780	708
Ca	2747	708

stechnik Berlin. This research was supported by the DFG under grant We 1312/2-3 and by the DARA under grant 50 OR 9409 1.

References

Anderson L.S. 1990. In: Properties of Hot Luminous Stars, Garmany C.D. (ed.) A.S.P. Conf. Ser. 7, p. 77
Auer L.H., Mihalas D. 1969, ApJ 158, 641
Auer L.H., Mihalas D. 1972, ApJS 24, 193
Bashkin S., Stoner J.O.Jr. 1975, Atomic Energy Levels And Grotrian Diagrams, North–Holland / American Elsevier
Becker S.R., Butler K. 1990a, A&A 235, 326
Becker S.R., Butler K. 1990b, A&AS 84, 95
Bues I., Aslan T. 1995. In: White Dwarfs, Koester D., Werner K. (eds.) Lecture Notes in Physics 443. Springer, Berlin, p. 259
Chayer P., Fontaine G., Wesemael F. 1995, ApJS 99, 189
Cunto W., Mendoza C. 1992, Rev. Mex. Astron. Astrofis. 23, 107
Dreizler S. 1993, A&A 273, 212
Dreizler S., Werner K. 1993, A&A 278, 199
Gehren T. 1975, A&A 38, 289
Grigsby J.A., Morrison N.D., Anderson L.S 1992, ApJS 78, 205
Haas S., Dreizler S., Heber U., Jeffery C.S., Werner K. 1996, A&A 331, 669
Heise J., Van Teeseling A., Kahabka P. 1994, A&A 288, L45
Holweger H. 1996, Physica Scripta in press
Holweger H. 1979, Les Elements et leurs Isotopes dans l'Univers, Universite de Liège, Inst. d. Astrophysique, p. 117
Hubeny I. 1992. In: Atmospheres of Early-Type Stars, Heber U., Jeffery C.S. (eds.) Lecture Notes in Physics 401. Springer, Berlin, p. 233
Hubeny I., Lanz T. 1993, IAU Coll. 138, A.S.P. Conf. Ser. 44, 98
Hubeny I., Lanz T. 1995, ApJ 439, 875
Hubeny I., Hummer D.G., Lanz T. 1994 A&A 282, 151
Husfeld D., Kudritzki R.P., Simon K.P.,Clegg R.E.S. 1984, A&A 134, 139
Hummer D.G., Mihalas D. 1988, ApJ 331, 794
Kamp L.W. 1973, ApJ 180, 447
Kudritzki R.P. 1976, A&A 52, 11
Kurucz R.L. 1979, ApJS 40, 1
Kurucz R.L. 1991. In: Stellar Atmospheres: Beyond Classical Models, Crivellari L., Hubeny I., Hummer D.G. (eds.) NATO ASI Series C 341, p. 441
Kurucz R.L. 1992. In: The Stellar Population of Galaxies, Barbuy B., Renzini A. (eds.) IAU Symp. 145. Kluwer, Dordrecht, p. 225
Lanz T., Hubeny I. 1995, ApJ 439, 905
Mihalas D. 1972, "Non-LTE Model Atmospheres for B and O stars", NCAR-TN/STR-76
Mihalas D. 1978, Stellar Atmospheres, Freeman, San Francisco
Moore C.E. 1971, Atomic energy levels Vol. I, NSRDS-NBS 35, U.S. Dept. of Commerce
Napiwotzki R., Rauch T. 1994, A&A 285, 603
Rauch T. 1993, A&A 276, 171
Rauch T. 1996. In: Supersoft X-ray Sources, Greiner J. (ed.) Lecture Notes in Physics 472. Springer, Berlin, p. 139
Rauch T., Werner K. 1988, A&A 202, 159
Rauch T., Werner K. 1991. In: Stellar Atmospheres: Beyond Classical Models, Crivellari L., Hubeny I., Hummer D.G. (eds.) NATO ASI Series C 341, p. 165
Rauch T., Heber U., Hunger K., Werner K., Neckel T. 1991, A&A 241, 457

Rentzsch-Holm I. 1996, A&A 312, 966
Schönberner D. 1983, ApJ 272, 708
Schöning T., Butler K. 1989, A&AS 78, 51
Seaton M.J. 1958, Rev. Mod. Phys. 30, 979
Seaton M.J. 1987, J. Phys. B 20, 6363
Seaton M.J., Zeippen C.J., Tully J. et al. 1992, Rev. Mex. Astron. Astrofis. 23, 19
Seaton M.J., Yu Yan, Mihalas D., Pradhan A.K. 1994, MNRAS 266, 805
Sedlmayr E. 1973, A&A 31, 23
Steenbock W., Holweger H. 1984, A&A 130, 319
Stürenburg S., Holweger H. 1990, A&A 237, 125
Takeda Y. 1995, PAPJ 47, 463
Werner K. 1986, A&A 161, 177
Werner K. 1988, A&A 204, 159
Werner K. 1989, A&A 226, 265
Werner K. 1996, ApJ 457, L39
Werner K., Husfeld D. 1985, A&A 148, 417
Werner K., Rauch T. 1994, A&A 284, L5
Werner K., Heber U., Hunger K. 1991, A&A 244, 437
Werner K., Rauch T., Dreizler S., Heber U. 1995. In: White Dwarfs, Koester D., Werner K. (eds.) Lecture Notes in Physics 443. Springer, Berlin, p. 171
Wiese W.L., Smith M.W., Glennon B.M. 1966, Atomic transition probabilities Vol. I, NSRDS-NBS 4, U.S. Dept. of Commerce
Wiese W.L., Smith M.W., Miles B.M. 1969, Atomic transition probabilities Vol. II, NSRDS-NBS 22, U.S. Dept. of Commerce

This article was processed by the author using Springer-Verlag LaTeX A&A style file *L-AA* version 3.